REVIEWS OF TOPICAL PROBLEMS　　　　　　　　　

Surface states in photonic crystals

A P Vinogradov, A V Dorofeenko, A M Merzlikin, A A Lisyansky

Contents

Abstract. The propagation of surface electromagnetic waves along photonic crystal (PC) boundaries is examined. It is shown that in a number of cases, these are backward waves. The nature of surface electromagnetic states localized at the PC boundary is discussed; these states transfer no energy along the boundary (their tangential wave number is zero). An analogy with the well-known Tamm and Shockley surface states in solid state physics is drawn. It is shown that in the case of a PC, both types of states can be regarded as Tamm states. Experimental results on the observation of surface states are presented. A system using an external magnetic field to control a surface state is considered.

1. Introduction

Recently, considerable attention in the literature has been focused on the investigation of the properties of photonic crystals (PCs) [1–3], which is primarily due to the prospect of their application in quantum optics and optoelectronics. However, the interaction of electromagnetic waves with PCs is also interesting from the standpoint of conventional natural-crystal optics. The main difference between PCs and conventional optical materials is as follows: in the passage of waves with wavelengths down to the ultraviolet range, homogeneous media can be considered continuous translation invariant, while PCs are invariant only under the group of discrete translations of the corresponding lattice.

A P Vinogradov, A V Dorofeenko, A M Merzlikin Institute for Theoretical and Applied Electromagnetics, Russian Academy of Sciences
ul. Izhorskaya 13, 125412 Moscow, Russian Federation
Tel. (7-495) 485 83 55
E-mail: alexandor7@gmail.com
A A Lisyansky Department of Physics, Queens College
of the City University of New York,
Flushin, New York 11367, USA

Under these conditions, highly unusual laws of refraction and reflection become applicable [4]. For instance, phenomena such as negative refraction, which is vigorously studied in metamaterials with a permittivity $\varepsilon < 0$ and a magnetic permeability $\mu < 0$ [5], the superprism effect [6–9], and the channeling of electromagnetic waves may be realized in PCs [10]. In the reflection from a high-index interface [11], side lobes may emerge even at low frequencies (the Borrmann effect) [12, 13], and leaky waves may emerge in the passage of waves through a bounded PC [14]. A close analogy between PC electrodynamics and quantum mechanics of ordinary electronic crystals plays an important role in the study of PC properties. It has enabled researchers to readily construct an adequate apparatus for the description of the phenomena by borrowing it from solid-state physics. In turn, the investigation of PCs has an impact on solid-state physics: the absence of the interaction between photons in linear electrodynamics allows studying the interference and diffraction effects in their pure form. These are Anderson localization [15], Berry oscillations [16–19], channeling [10], and emergent surface states, which are the subject of our review. In finite samples of homogeneous media, as well as of PCs, surface solutions localized on both sides of the boundary emerge [20–22] because the boundary breaks the translational invariance.

In the recent literature concerned with PCs, a tendency can be seen to draw a distinction between Tamm and Shockley surface states in PCs [23–25]. In this review, we consider both of them in detail and show that there are no special reasons to distinguish between these states because the physics underlying their occurrence is the same.

For clarity and for simplicity of computations, our consideration is based on one-dimensional PCs (layered systems). In the simplest case of isotropic materials, this is a physical realization of the Kronig–Penney model. However, the vector nature of fields in electrodynamics makes the one-dimensional problem much richer than the quantum-mechanical one. This difference is most clearly exposed in the consideration of PCs consisting of anisotropic materials.

2. Surface solutions at the interface between homogeneous media

We begin with the problem of the propagation of surface electromagnetic waves. As is commonly known [22, 26, 27], a surface wave may propagate along the boundary between isotropic media whose permittivities have opposite signs. The field of this wave decreases exponentially with the distance from the interface. The field decrease in a medium with a negative permittivity (NP) is due to the purely imaginary value of the wavenumber in this medium. The wave decrease in a medium with a positive permittivity is due to the condition for total internal reflection: the tangential component of the wave vector of a surface wave (SW) exceeds in modulus the wave vector $k_{>0}$ in the medium with positive permittivity $\varepsilon_{>0}$ (see Ref. [22]):

$$k_x^2 = k_0^2 \frac{|\varepsilon_{<0}|\varepsilon_{>0}}{|\varepsilon_{<0}| - \varepsilon_{>0}} > k_0^2 \varepsilon_{>0}. \tag{1}$$

It is noteworthy that the SW under consideration is TM polarized (Fig. 1a). If a medium with a negative magnetic permeability (NMP) is taken instead of an NP medium, the SW is TE polarized.

The Poynting vectors on different sides of the interface are oppositely directed [27], such that the Poynting vector is antiparallel to the phase velocity in the NP medium (NMP medium) and is parallel to the phase velocity in the medium with positive permittivity and permeability. The total energy transfer is aligned with the phase velocity: the SW is a direct wave.

In addition to surface waves, other solutions localized near the interface may exist. At the interface between an NP medium and an NMP medium, a surface state exists with a zero wavenumber along the surface if $\mu_1/\varepsilon_1 = \mu_2/\varepsilon_2 < 0$ [28, 29].

The requirement that the permittivity changes sign in passing through the interface is needed to match the continuity condition for the tangential field components to the exponential field decrease on both sides of the interface.
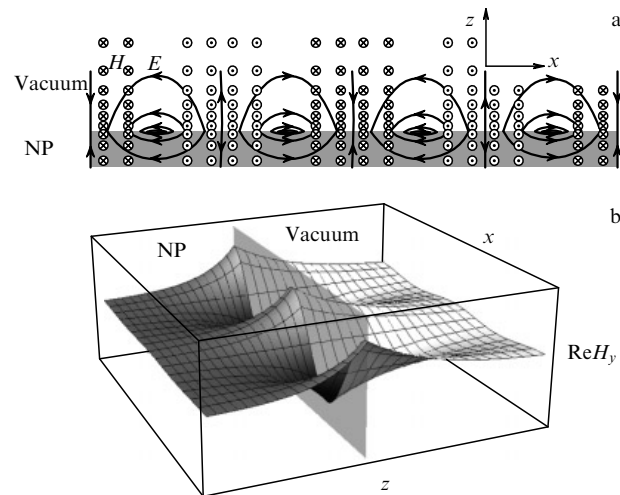

Figure 1. Surface wave at the interface between two homogeneous media ($\varepsilon_1 = 1$, $\varepsilon_2 = -2$). (a) Electric and magnetic field lines near the surface (the medium with $k_x/k_0 = 1.414$ is on top). (b) Coordinate dependence of the magnetic field. The wave parameters is $k_x/k_0 = 1.414$.

The continuity of the tangential electric field component $E_x \sim (1/\varepsilon)(\partial H_y/\partial z)$ requires compensation of the change of sign of the derivative $\partial H_y/\partial z$, which occurs due to the exponential decrease in the magnetic field with the distance from the interface (Fig. 1b).

3. Surface waves at the boundary of a photonic crystal

PCs are noted for a wide variety of different surfaces modes. The underlying reason is the difference between Bloch and plane waves. While the propagation of a Bloch wave over distances greater than the elementary cell size is well described by the Bloch wave vector, a substantial difference in the field distribution between plane and Bloch waves occurs on a scale smaller than the elementary cell size, even though the wave vectors of these waves may coincide.

For example, we consider a PC whose cell consists of two homogeneous layers (Fig. 2). In the general case of an oblique wave propagation with respect to the PC plane that is perpendicular to the z axis, the problem is two-dimensional and reduces to two scalar problems that correspond to the TE polarization (with the nonzero field components E_y, H_x, and H_z) and the TM polarization (with the nonzero field components H_y, E_x, and E_z) [30]. For the TE polarization, the electric and magnetic fields of these waves in the nth layer are given by

$$\begin{aligned}
E_{yn} &= A_n \exp\left[ik_{zn}(z - z_n) + ik_x x\right] \\
&\quad + B_n \exp\left[-ik_{zn}(z - z_n) + ik_x x\right], \\
H_{xn} &= i\frac{c}{\omega}\frac{\partial}{\partial z} E_y = -\frac{c}{\omega} k_{zn}\Big\{A_n \exp\left[ik_{zn}(z - z_n) + k_x x\right] \\
&\quad - B_n \exp\left[-ik_{zn}(z - z_n) + ik_x x\right]\Big\}, \\
H_{zn} &= -i\frac{c}{\omega}\frac{\partial}{\partial x} E_y = \frac{c}{\omega} k_{xn}\Big\{A_n \exp\left[ik_{zn}(z - z_n) + ik_x x\right] \\
&\quad + B_n \exp\left[-ik_{zn}(z - z_n) + ik_x x\right]\Big\},
\end{aligned} \tag{2}$$

where z_n is one of the boundaries of the nth layer and $k_{zj} = (\varepsilon_j \mu_j k_0^2 - k_x^2)^{1/2}$ is the normal component of the wave vector in the jth layer.

We use the continuity condition for E_y and H_x at the layer boundary and invoke the Floquet theorem ($E(z + d) = \exp(ik_B d) E(z)$, where k_B is the Bloch wavenumber) to obtain a homogeneous system of linear equations for the coefficients A_n and B_n [31–35]. The condition that the determinant of the corresponding matrix vanishes leads to a dispersion equation that defines the Bloch wavenumber. When the cell consists of two layers, the equation has the
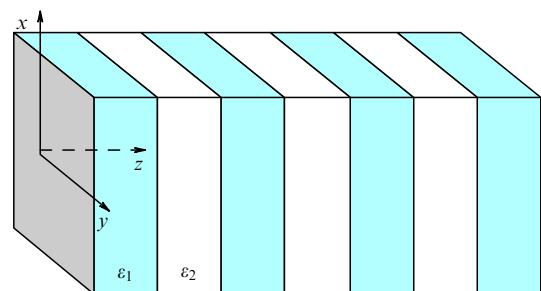

Figure 2. Schematic diagram of a one-dimensional photonic crystal.

form [31–35]

$$\cos\left[k_{\mathrm{B}}(d_1 + d_2)\right] = \cos(k_{z1}d_1)\cos(k_{z2}d_2)$$
$$- \frac{1}{2}\left(\frac{\zeta_1}{\zeta_2} + \frac{\zeta_2}{\zeta_1}\right)\sin(k_{z1}d_1)\sin(k_{z2}d_2), \qquad (3)$$

where the indices 1, 2 denote the layer number and ζ_n is the normal impedance [1] of a layer [32]. For the TM polarization, $\zeta_n = k_{zn}/(k_0\varepsilon_n)$, and for TE polarization, $\zeta_n = -(k_0\mu_n)/k_{zn}$. [2]

It is important for the subsequent analysis that although Eqn (3) defines the effective wavenumber k_{B} of a Bloch wave propagating through a PC, assigning this wave the effective characteristic or normal impedance is impossible. This is because the ratio between the fields is uniquely related to these quantities only for a plane wave propagating through a homogeneous space. In every individual layer of a PC, the Bloch wave is the sum of two counterpropagating plane waves [31, 32, 34]. As a result, the ratio $\zeta = E_{\mathrm{t}}/H_{\mathrm{t}}$ varies even within one layer. In general, this ratio is a periodic function of the coordinate, which distinguishes the Bloch wave from the plane one, for which the ratio $\zeta = E_{\mathrm{t}}/H_{\mathrm{t}}$ has no spatial dependence.

When the modulus of the right-hand side of Eqn (3) exceeds unity at some frequency, k_{B} acquires an imaginary part, and there are no bounded solutions for an infinite PC. These frequencies make up a forbidden band. When a PC fills a semi-infinite space, bounded solutions exist at the frequencies of the forbidden band; on average, these solutions decrease exponentially with the distance from the boundary. We emphasize that the Bloch wave does not transfer energy in the forbidden band and that its impedance is a purely imaginary quantity (we neglect losses). Being a periodic function of the coordinate normal to the interface, the quantity $\zeta = E_{\mathrm{t}}/H_{\mathrm{t}}$ takes all values from $-\mathrm{i}\infty$ to $+\mathrm{i}\infty$ within a PC cell (Fig. 3) and is equal to the input impedance of a semi-infinite PC whose boundary coincides with the corresponding cell section. Therefore, ζ takes any purely imaginary value, depending on the choice of the location of the elementary cell boundary. At the lower edge of the forbidden band, the pole of the input impedance is observed when the elementary cell boundary passes through the middle of the higher-ε layer (the solid line in Fig. 3). As the frequency increases, the pole shifts, and at the frequency of the upper edge of the forbidden band, it is located in the middle of the lower-ε layer (the dashed line in Fig. 3).

The zero or infinite impedance values occur at the positions of the electric and magnetic field nodes that appear in the prefactor of the Bloch wave at forbidden band frequencies. In the general case, the input impedance may take any intermediate value, depending on the location of the PC boundary. This ensures the existence of surface waves at the interface between a PC and a medium with positive permittivity and permeability. When the condition for total internal reflection is satisfied, the solution in the medium with
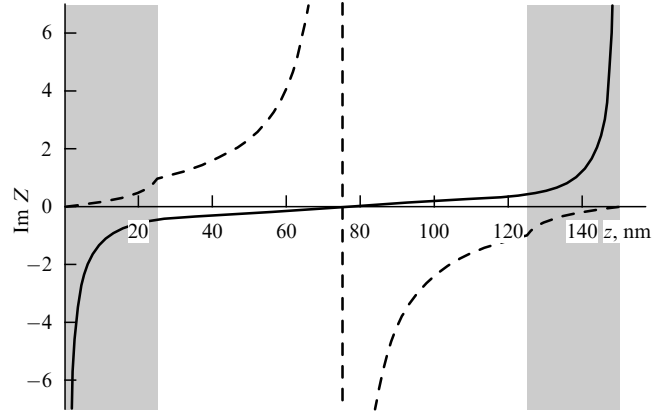

Figure 3. Coordinate dependence of the imaginary part of the impedance within one elementary PC cell of the form $\{(\varepsilon_1, d_1/2), (\varepsilon_2, d_2), (\varepsilon_1, d_1/2)\}$ for the lower (solid curve, frequency $k_0 = 0.00807\ \mathrm{nm}^{-1}$) and upper (dashed curve, frequency $k_0 = 0.0159\ \mathrm{nm}^{-1}$) edges of the first forbidden band for $k_x = 0$. The higher-permittivity layer is shown in dark color. The real part of the impedance is equal to zero because there is no energy transfer. The parameters are $\varepsilon_1 = 10$, $\varepsilon_2 = 1$, $d_1 = 50\ \mathrm{nm}$, $d_2 = 100\ \mathrm{nm}$.

positive permittivity and permeability decreases exponentially with the distance from the interface and has a purely imaginary surface impedance at the interface. This solution may be matched to the Bloch wave. This matching becomes possible due to the oscillations of the Bloch wave field inside the elementary cell. They have the effect that the sign of $\partial H_y/\partial z$ may be positive at isolated points, despite the exponential wave decay on the scale of an integer number of cells, while the decreasing exponent by itself has a negative derivative (Fig. 4) (see Ref. [36]).

The dispersion equation of a surface wave is the previously mentioned condition for the equality of surface impedances of waves that decrease with the distance from the interface of a uniform medium and a photonic crystal.
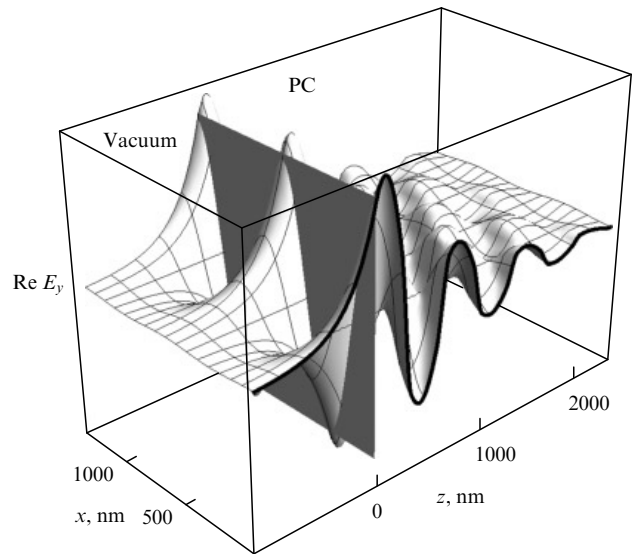

Figure 4. TE-polarized surface wave (the instantaneous value of the electric field) at the interface between the vacuum and a PC with the cell $\{(\varepsilon_1, d_1), (\varepsilon_2, d_2)\}$ ($\varepsilon_1 = 2$, $\varepsilon_2 = 10$, $d_1 = 232\ \mathrm{nm}$, $d_2 = 100\ \mathrm{nm}$, and frequency $k_0 = 0.00835\ \mathrm{nm}^{-1}$). The tangential wave vector component is such that $k_x/k_0 = 0.8\sqrt{\varepsilon_1}$, which ensures wave propagation in every PC layer and an exponential decrease in the vacuum.

---

[1] The characteristic impedance $\sqrt{\mu/\varepsilon}$ must be distinguished from the normal impedance, which appears in the problem of plane wave refraction at the boundary of a semi-infinite space filled with a homogeneous material. These impedances coincide only in the case of normal incidence.
[2] We emphasize that for the TE polarization, the normal impedance, which is defined as the ratio $E_{\mathrm{t}}/H_{\mathrm{t}}$, is a negative quantity equal to the negative value of the impedance ζ_L, which is introduced by the equality $E_{\mathrm{t}} = \zeta_L \mathbf{H} \times \mathbf{n}$ [22], because when $\mathbf{n} = (0, 0, 1)$, this definition yields $E_y = -\tau_L H_x$.

For a crystal with a cell consisting of two uniform layers, it follows from Eqns (2) and (3) that the surface impedance Z for the TM polarization, or the surface admittance (the inverse impedance) for the TE polarization, is given by [36]

$$
Z = -\zeta_1 \Big\{ (\zeta_2 \cos k_{z1} d_1 + i\zeta_1 \sin k_{z1} d_1) \exp (i k_{z2} d_2)
$$
$$
- \zeta_2 \exp \big[i k_{\mathrm{B}} (d_1 + d_2) \big] \Big\}
$$
$$
\times \Big\{ (\zeta_1 \cos k_{z1} d_1 + i\zeta_2 \sin k_{z1} d_1) \exp (i k_{z2} d_2)
$$
$$
- \zeta_1 \exp \big[i k_{\mathrm{B}} (d_1 + d_2) \big] \Big\}^{-1} , \qquad (4)
$$

where $\zeta_j = k_{zj}/(\varepsilon_j k_0)$ is the normal impedance in the jth layer for the TM polarization and $\zeta_j = -k_{zj}/(\mu_j k_0)$ is the normal admittance in the jth layer for the TE polarization.

The wave in a homogeneous semi-infinite space located to the left of the PC should decrease in the negative direction of the z axis, and hence the wavenumber corresponding to it is $-k_z$ and the surface impedance is equal to the negative value of the normal impedance.

By equating the surface impedances, we obtain the condition for the existence of a TE-polarized surface wave [31]:

$$
\frac{\sqrt{\varepsilon \mu k_0^2 - k_x^2}}{\mu} = \frac{k_{z1}}{\mu_1} \left\{ \left[\frac{k_{z2}}{\mu_2} \cos(k_{z1} d_1) + i \frac{k_{z1}}{\mu_1} \sin(k_{z1} d_1) \right] \right.
$$
$$
\times \exp (i k_{z2} d_2) - \frac{k_{z2}}{\mu_2} \exp \big[i k_{\mathrm{B}} (d_1 + d_2) \big] \right\}
$$
$$
\times \left\{ \left[\frac{k_{z1}}{\mu_1} \cos(k_{z1} d_1) + i \frac{k_{z2}}{\mu_2} \sin(k_{z1} d_1) \right] \right.
$$
$$
\left. \times \exp (i k_{z2} d_2) - \frac{k_{z1}}{\mu_1} \exp \big[i k_{\mathrm{B}} (d_1 + d_2) \big] \right\}^{-1} \qquad (5)
$$

with $k_{z1} = \sqrt{\varepsilon_1 \mu_1 k_0^2 - k_x^2}$ and $k_{z2} = \sqrt{\varepsilon_2 \mu_2 k_0^2 - k_x^2}$, and the condition for the existence of a TM-polarized surface wave:

$$
\frac{\sqrt{\varepsilon \mu k_0^2 - k_x^2}}{\varepsilon} = \frac{k_{z1}}{\varepsilon_1} \left\{ \left[\frac{k_{z2}}{\varepsilon_2} \cos(k_{z1} d_1) + i \frac{k_{z1}}{\varepsilon_1} \sin(k_{z1} d_1) \right] \right.
$$
$$
\times \exp (i k_{z2} d_2) - \frac{k_{z2}}{\varepsilon_2} \exp \big[i k_{\mathrm{B}} (d_1 + d_2) \big] \right\}
$$
$$
\times \left\{ \left[\frac{k_{z1}}{\varepsilon_1} \cos(k_{z1} d_1) + i \frac{k_{z2}}{\varepsilon_2} \sin(k_{z1} d_1) \right] \right.
$$
$$
\left. \times \exp (i k_{z2} d_2) - \frac{k_{z1}}{\varepsilon_1} \exp \big[i k_{\mathrm{B}} (d_1 + d_2) \big] \right\}^{-1} . \qquad (6)
$$

When ε and μ are positive in a homogeneous medium bordering a PC, such waves localized near the PC boundary are bound to have a nonzero tangential wavenumber, because the formation of an inhomogeneous wave in a homogeneous space requires the condition for total internal reflection. The existence of an SW on the PC surface does not necessitate the existence of a boundary at which the permittivity or the permeability change sign. While the exponential decrease in the SW in a homogeneous semi-infinite space is related to the condition of total internal reflection ($k_x^2 > k_0^2$), the decrease in the SW field in the direction to the interior of the PC is related to the existence of a forbidden band. In this case, the PC plays the role of a medium with negative permittivity (permeability). We note that the SW at the interface with a PC with positive permittivity and permeability exists when the solution in at least one of the layers is a propagating solution ($k_0^2 \varepsilon_i > k_x^2$) [31].

We note that a PC can maintain both TE and TM SWs within one forbidden band, playing the role of either a negative-permittivity medium or a negative-permeability medium [36]. Because the TE- and TM-forbidden bands do not generally coincide for nonzero values of the tangential wavenumber, for greater clarity we consider the band structure of a class of PCs with different first-layer thicknesses d_1. We fix the value of $\gamma = k_x/k_0$ and introduce the parameter

$$
D_1 = \frac{d_1 \sqrt{\varepsilon_1 - \gamma^2}}{d_1 \sqrt{\varepsilon_1 - \gamma^2} + d_2 \sqrt{\varepsilon_2 - \gamma^2}} ,
$$

which has the meaning of the relative optical thickness of the first layer and characterizes the PC cell structure. In Fig. 5, the bands allowed for both polarizations are marked in dark grey, the TE-forbidden bands in light grey, and the TM-forbidden bands in white. It can be seen that TM-forbidden bands are inside the TE-forbidden bands. The solid bold and dotted lines respectively correspond to surface waves with the TE and TM polarizations. Therefore, for the same PC (with the value of D_1 fixed) and the same forbidden band number, we can observe SWs with both polarizations, although at different frequencies. When the values of $\gamma = k_x/k_0$ for TE and TM polarizations are different, it is possible to obtain SWs with both polarizations at the same frequency, but they then reside in forbidden bands with different numbers.

As discussed above, an SW can propagate at the interface between homogeneous media when $|\varepsilon_{<0}| > \varepsilon_{>0}$. Although the Poynting vector in an NP medium is antiparallel to the phase velocity of the SW, this inequality makes the surface wave direct (the total Poynting vector is parallel to the phase velocity of the SW). In the case of a PC–NP-medium interface (with the PC acting as a medium with positive permittivities), the above bound on the permittivities is absent, which has the consequence that the backward SW may exist (both the total Poynting vector and the group velocity are antiparallel to the
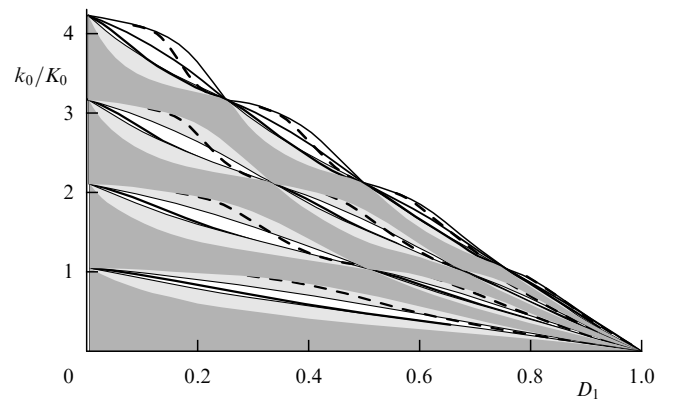

Figure 5. Evolution of the PC band structure as D_1 varies. The bands forbidden for TM-polarized waves (shown in white) are inside the bands forbidden for TE-polarized waves (shown in light grey and white). Dashed and bold solid lines respectively correspond to TE and TM surface waves. The abscissa shows the relative optical thickness D_1 of the first layer. The PC cell parameters $\{(\varepsilon_1, d_1), (\varepsilon_2, d_2)\}$ are $\varepsilon_1 = 2$, $\varepsilon_2 = 10$, $\varepsilon_{\mathrm{ext}} = 1$, the value $\gamma = k_x/k_0 = 0.8\sqrt{\varepsilon_1} k_0$ ensures propagation through the dielectric with a permittivity ε_1 and an exponential decrease in the vacuum required for the existence of a surface wave. The frequency is normalized by the quantity $K_0 = \pi/(d_2 \sqrt{\varepsilon_2 - \gamma^2})$.
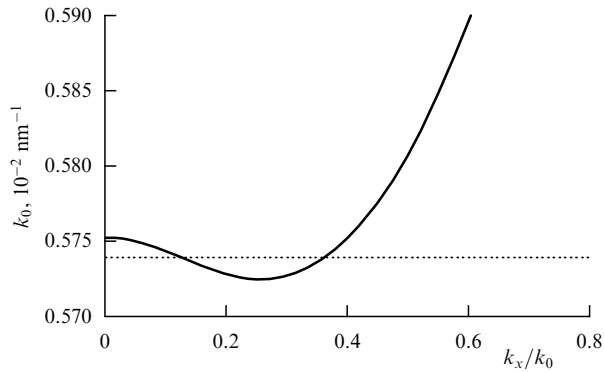
Figure 6. Dispersion curve for a TM-polarized surface state from the first forbidden band of a PC with the cell $\{(\varepsilon_1, d_1), (\varepsilon_2, d_2)\}$ where $\varepsilon_1 = 2$, $\varepsilon_2 = 10$, $d_1 = 200$ nm, and $d_2 = 100$ nm, which has an interface with an NP medium with $\varepsilon = -0.1$. The negative slope of the dispersion curve corresponds to a backward wave.

Figure 7. Tamm state at the interface between a PC (for which $\varepsilon_1 = 2$, $\varepsilon_2 = 1$, $d_1 = d_2 = 100$ nm, $k_0 = 0.0132$ nm^{-1} is the frequency of the Tamm state, and the cell is symmetric $\{(\varepsilon_1, d_1/2), (\varepsilon_2, d_2), (\varepsilon_1, d_1/2)\}$) and a medium with $\varepsilon_{\mathrm{SNG}} = -3$. The tangential component of the wave is vector $k_x = 0$.

phase velocity of the SW). This situation is illustrated in Fig. 6. The existence of a negative-slope portion of the dispersion curve (see Fig. 6) signifies that two surface waves may exist at the same frequency for different values of k_x: one of the waves is direct and the other is backward. In one wave, more energy is transferred through the PC, and in the other, through the NP medium.

The existence of backward surface waves was first considered in papers studying SWs at the interface between a PC and a Veselago medium (a medium with negative permittivity and negative permeability) [37–39]. As follows from the foregoing, the negativeness of only one of them would be sufficient for the existence of backward SWs; however, backward SWs with only one polarization may be observed in that case: TM for an NP medium and TE for an NMP medium.

4. Tamm surface states

The surface waves considered in Section 3 travel along the interface between a PC and a medium with positive permittivity and permeability. By combining two such waves traveling in opposite directions, it is possible to obtain a state in the form of a standing surface wave, which does not transfer energy. In this case, the tangential wavenumber k_x is not equal to zero, because the condition for total internal reflection in the dielectric bordering the PC should be satisfied. However, when a PC made of nonmagnetic dielectrics has an interface with an NP material, this condition does not have to be satisfied, and solutions with $k_x = 0$ may exist on the boundary that are uniform along the surface (surface states) and do not transfer energy (Fig. 7). [3] Using the analogy to the previously mentioned Engheta surface state [28] at the interface between NP and NMP media, the PC may be considered a medium with $\mu < 0$.

We also note that the equation for the electric field is an exact analog of the one-electron Schrödinger equation for a semi-infinite crystal, whose solution is the Tamm surface

state [36]. [4] In this case, the Maxwell equations reduce to the Helmholtz equation

$$\frac{\partial^2}{\partial z^2} E_y + k_0^2 \varepsilon E_y = 0, \qquad (7)$$

and the boundary conditions require the continuity of E_y and H_x. Because $H_x \sim \partial E_y/\partial z$, there is the complete correspondence with the quantum mechanical problem

$$\frac{\partial^2 \psi}{\partial z^2} + \frac{2m(E - U)}{\hbar^2} \psi = 0,$$

where ψ and $\partial \psi/\partial z$ are continuous at the boundary.

In the general case, the dispersion equation for the surface state under consideration is defined by formula (5) with $k_x = 0$.

We emphasize that we are dealing with a solution having a zero tangential wavenumber. Only surface waves could exist in all the above systems composed only of materials with positive ε and μ. Exciting these waves by an incident wave requires a prism or a diffraction grating to ensure the total reflection condition. Here, we are dealing with a surface state (Fig. 10), which may be observed when a wave is incident on the layers normally [26]. The Tamm state may be experimentally discovered by measuring the wave transmittance of a finite-thickness photonic crystal layer interfaced with a material layer with $\varepsilon < 0$. At the frequency corresponding to the Tamm state, a narrow transmittance peak (Fig. 8) arising from the tunneling of light through the Tamm state is observed [36, 44]. The transmittances of the homogeneous layer alone and of the PC (at a frequency in the forbidden band) alone, indeed, turn out to be much lower than the transmittance of the coupled system (see Fig. 8), because on

---

[3] The possible existence of uniform surface states that do not transfer energy was first considered in Refs [40, 41], where the problem of a PC at an interface with a perfectly conducting surface was solved. Among the waveguide-type solutions, a solution with $k_x = 0$ was found. However, this fact did not receive proper attention (see Fig. 10).
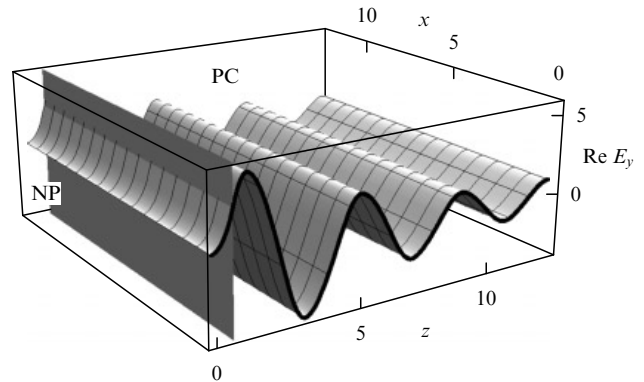
[4] In 1932, Tamm [42] predicted a new quantum effect: the localization of an electron near the surface of a crystal. While the localization of a classical particle requires that the potential energy have a well in some specific spatial domain and the height of the potential barrier at the edges of the domain exceed the total particle energy, a quantum particle may be 'stopped' by a periodic potential even in the case of above-barrier reflection. The treatment was performed in the framework of the Kronig–Penney model. The role of negative permittivity was played by the external potential, which exceeded the energy of the Tamm state (see, e.g., Ref. [43]).
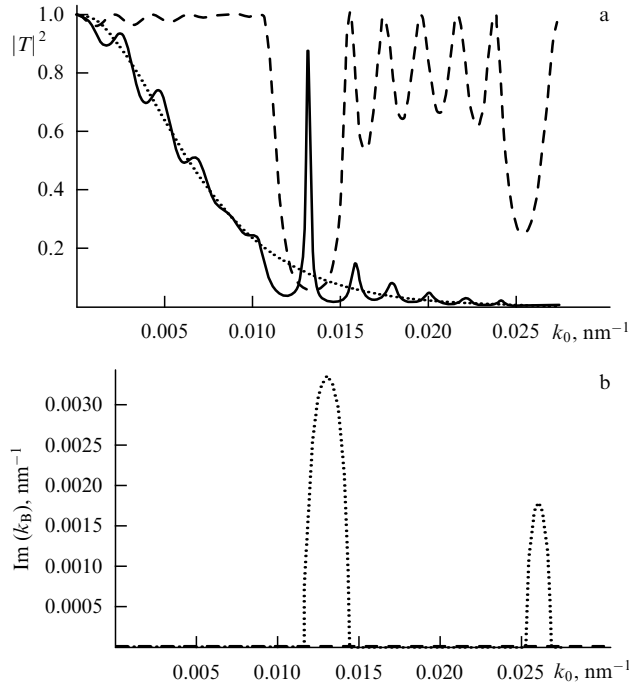
Figure 8. Tamm state at the interface between a PC (6 periods) and an NP medium (thickness $d_{SNG} = 709$ nm), with the same parameters as in Fig. 7. (a) Transmittance of the system of the PC and a homogeneous medium (solid curve) as well as of the PC (dashed curve) and of the layer of the homogeneous medium (dotted curve) taken separately. (b) Imaginary part of k_B, which defines the location of forbidden bands in the crystal. At the frequency $k_0 = 0.0132$ nm^{-1}, the transmission of a wave residing in the forbidden band of the crystal is observed.

average the light is exponentially attenuated in passing through the PC or the NP medium.

We recall that a PC may act as both an NP medium and an NMP medium. This has the consequence that surface states may exist at the interface between two different PCs (Fig. 9) [36, 44–51].

Clearly, such a state lies in the frequency range corresponding to the intersection of the forbidden bands of these crystals. This state attracts particular interest because it does not require the existence of media with negative ε or μ.
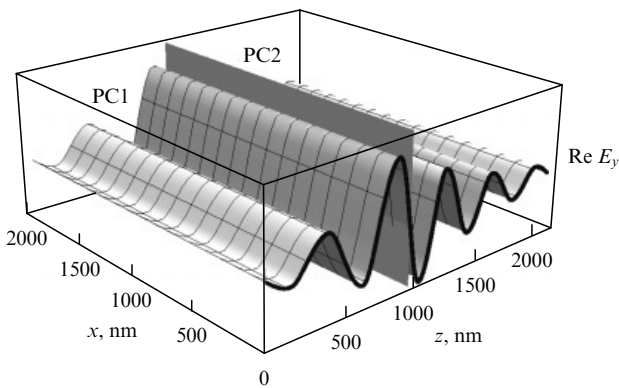

Figure 9. Tamm state at the interface between two PCs (parameters of the first PC are $\varepsilon_1 = 1$, $\varepsilon_2 = 4$, $d_1 = 157$ nm, $d_2 = 91$ nm; parameters of the second PC are $\varepsilon_1 = 4$, $\varepsilon_2 = 2$, $d_1 = 79$ nm, $d_2 = 111$ nm). The wave number is $k_0 = \omega/c = 0.01$ nm^{-1} and the tangential component of the wave vector is $k_x = 0$.
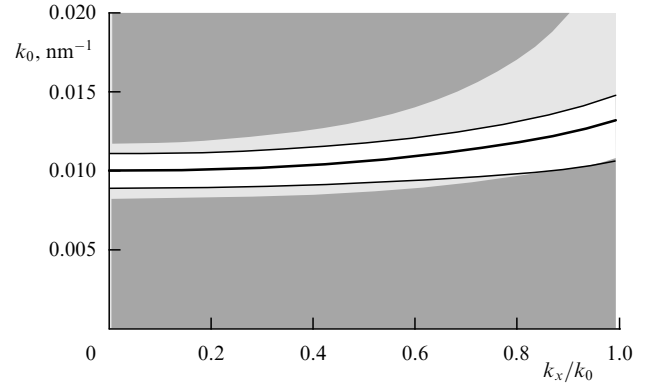

Figure 10. Frequency of a TE-polarized SW propagating along the interface between two PCs as a function of the tangential wavenumber k_x (bold curve). The solution with $k_x = 0$ signifies the existence of a surface state. The common forbidden band of the photonic crystals is shown in white. The allowed bands are marked in grey, the darker color corresponds to the first PC (the PC parameters are specified in the caption to Fig. 9).

The equation that defines the parameters of this state corresponds to the equality of surface impedances of waves in both crystals. These quantities are calculated by formula (4) with $k_x = 0$. Both Bloch wavenumbers should be complex and the waves should decrease away from the boundary.

In the system of two interfaced photonic crystals, the existence of a Tamm state may be experimentally discovered by observing the peak of transmittance of a sample consisting of finite PC pieces, at the frequencies of the overlap of the forbidden bands of the crystals (Fig. 11).

The existence of a Tamm surface state at the interface between two PCs was experimentally observed in Ref. [44]. The first PC samples consisted of five bilayer elementary cells, each of them comprising a 138 nm thick SiO_2 layer and a 93.6 nm thick Ta_2O_5 layer. The elementary cell of the second PC comprised an 87 nm thick magnetooptical layer of bismuth-substituted yttrium iron garnet and a 138 nm thick SiO_2 layer (Fig. 12). In the experiment, the transmittance and the Faraday rotation angle for transmitted wave polarization were measured (Fig. 13).

The characteristic transmission peak observed in the experiment is in agreement with theoretical predictions that attribute this peak to the existence of a surface state (SS).

Interestingly, when a PC is magnetized, the permittivity of layers made of a magnetooptical material assumes the form of a gyrotropic tensor. As a consequence, the eigensolutions of the Maxwell equations inside a magnetooptical layer are circularly polarized waves with different wavenumbers [52]. This results in the removal of the polarization degeneracy of Bloch waves and in the emergence of two SSs close in frequency, while the resonance transmission of differently polarized waves is observed at different frequencies. An enhancement of the Faraday effect, as in the presence of a defect, is observed at the frequency lying halfway between these resonances [36, 53, 54] (Fig. 13b).

5. Shockley's approach

Tamm's work on surface states [20, 42] gave rise to a number of papers [21, 55–61] (see also review [43]) where various models of semi-infinite or bounded crystals were considered under different approximations. In 1939, Shockley [21] followed the evolution of eigenstates of a finite chain of one-
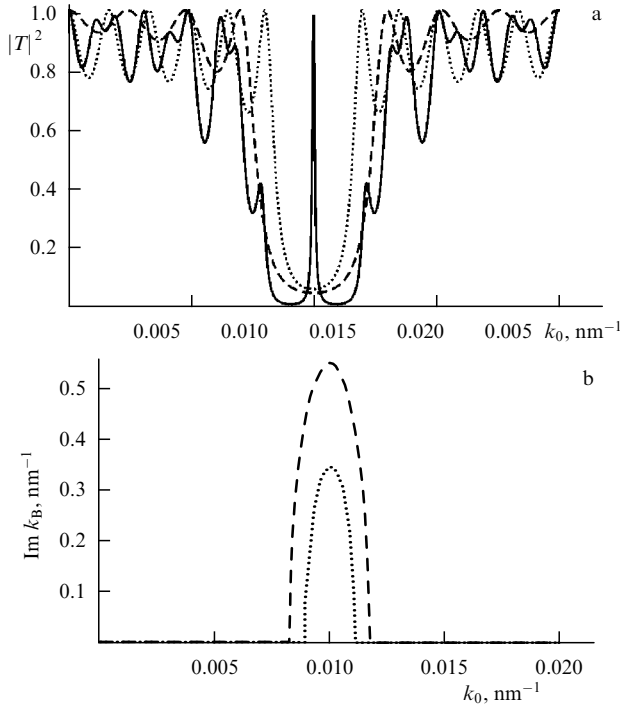
Figure 11. Transmittance of the system of two PCs (the parameters are the same as in Fig. 9). (a) Transmittance of the system of two crystals (solid curve) and of each of the crystals separately (dashed and dotted curves). (b) Imaginary part of k_B for the two crystals. At the frequency $k_0 = 0.01$ nm^{-1}, the transmission of a wave located in the forbidden band of the crystal is observed.

Figure 12. (a) Photograph of the structure used in the experiment. (b) Coordinate dependence of the permittivity and the calculated field distribution in the structure.
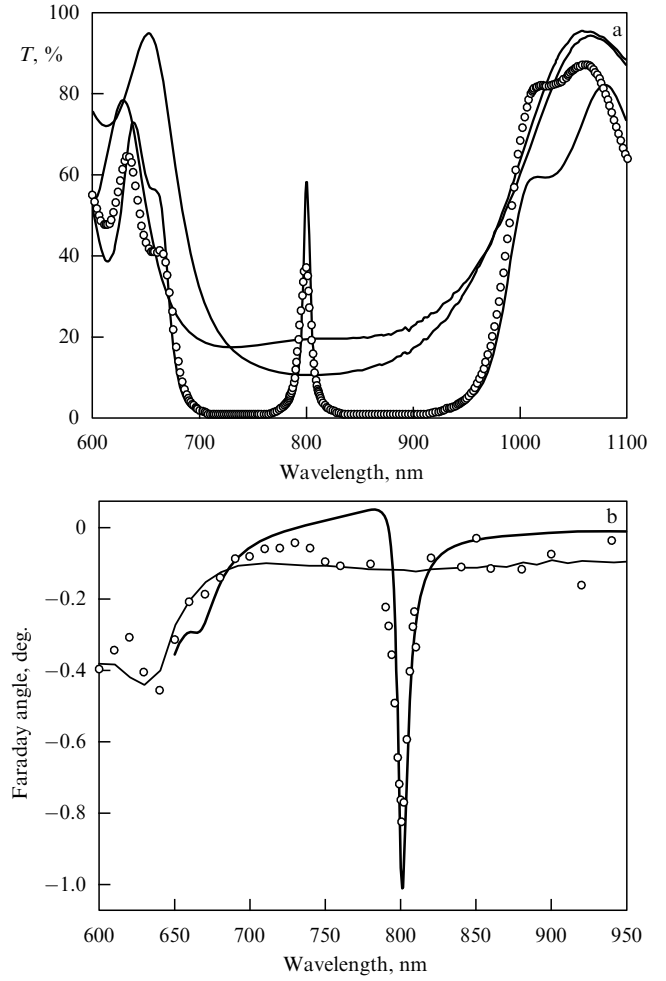

Figure 13. Calculated (solid curves) and experimental (circles) data. (a) Transmittance of the PC/PC structure (the curve with a peak) and of each of the two separate PCs. (b) Faraday angle for the PC/PC structure (the curve with a peak) and for a homogeneous Bi:YIG layer of summary thickness.
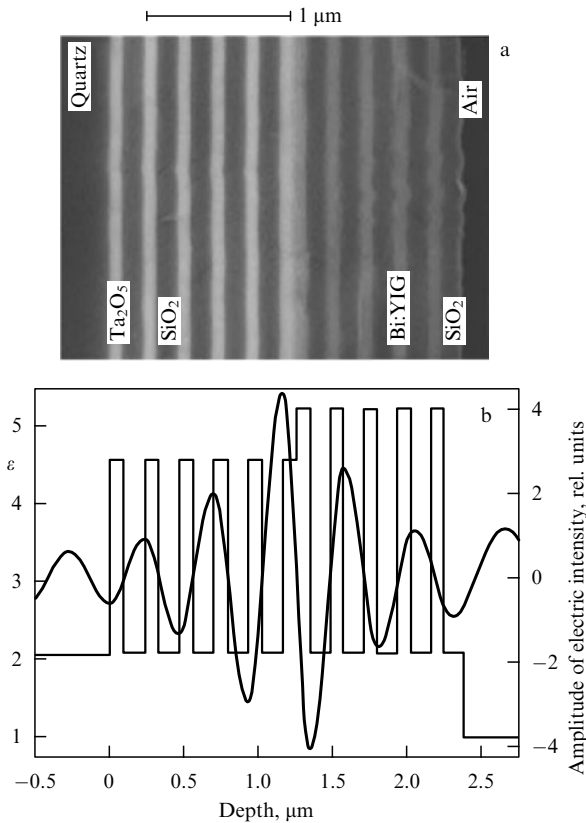
dimensional atoms as the distance between them decreased, and predicted the formation of SSs from the atomic states. In his opinion, the nature of the SSs was different from the nature of Tamm states. According to Shockley, the new SSs were formed due to the intersection of s- and p- bands. Furthermore, the significant effect of boundary conditions was emphasized. Allegedly, a perturbation of the potential at the boundary was necessary for the formation of Tamm states, while this was not required for the formation of the new Shockley states.

The states obtained by Shockley emerge even in the framework of the equations of a one-electron problem, but to interpret their nature, Shockley resorted to the properties of a many-electron system obeying the Fermi statistics, i.e., imposed additional constraints on the solutions not stemming from the initial equations. Therefore, despite several subtle points observed by Shockley, paper [21] did not give a clear criterion for distinguishing between Tamm and Shockley states [62, 63]. As a consequence, this paper by Shockley generated a multitude of attempts to derive this criterion. In particular, explanations emerged that attributed Shockley states to the formation of dangling bonds at the crystal boundary [64, 65].

The condition for the existence of a PC surface state requires an exponential field decrease with increasing the distance from the interface. It follows from the foregoing that there are only three possible reasons for such behavior: the fulfillment of the total internal reflection condition (which gives rise to surface waves), the existence of a purely imaginary wavenumber in NP and NMP media, and the existence of a forbidden band. Do Shockley's requirements give rise to a new mechanism?

We begin with the 'intersection of transparency bands.' Actually, what is important is not the intersection of transparency bands [21, 66] but the intersection of the edges of these bands. More recently [67, 68], this effect was interpreted as the intersection of the edges of a forbidden band separating transparency bands or, more precisely, as the closing of the transparency bands and the formation of a zero forbidden band. The essence of the effect is easiest to understand in the example of a PC with the elementary cell consisting of two layers. It turns out that when the optical layer thicknesses are multiples of each other, their transparency conditions (the conditions for the optical path to be equal to an integer number of wavelengths) may be satisfied simultaneously:

$$d_1 \sqrt{\varepsilon_1} k_0 = \pi n_1 \,,$$
$$d_2 \sqrt{\varepsilon_2} k_0 = \pi n_2 \,.$$

In this case, although the Bragg reflection condition required for the formation of a forbidden band is satisfied,

$$d \langle k \rangle = \pi n \,,$$

where $d = d_1 + d_2$, $\langle k \rangle = (d_1 \sqrt{\varepsilon_1} k_0 + d_2 \sqrt{\varepsilon_2} k_0)/(d_1 + d_2)$, and $n_1 + n_2 = n$, the forbidden band itself is not formed: the T-matrix of the elementary cell is equal to the unit matrix up to a sign (for more details, see Refs [67–70]), i.e., a wave incident on the cell does not experience reflection. It is noteworthy that for the simplest, two-layer cell, this effect is possible only in the case of above-barrier scattering. For a more complex potential like that used in Shockley's work, a forbidden band may close in the presence of small tunneling segments, which emerge when the interatomic distance is sufficiently long.

Although the effect of a zero forbidden band by itself does not give rise to a new mechanism of state localization near the crystal boundary, we show in what follows that it plays an important role in the possible classification of Tamm surface states as Shockley and non-Shockley states.

We now consider the problem of the necessity of 'potential perturbation at the boundary' in greater detail. It is commonly assumed that Shockley states exist in the absence of this perturbation, and that Tamm states emerge for a sufficiently strong perturbation (as this takes place, the Shockley states may also exist) [23, 24, 71, 72]. We note that a perturbation of boundary conditions (deposition of additional layers on the boundary, and so on) may change the surface state frequency and the picture of the evolution as the 'atoms' approach one another, but not the physics of the phenomenon. No new mechanism responsible for the exponential field decrease with the distance from the surface emerges. [5]
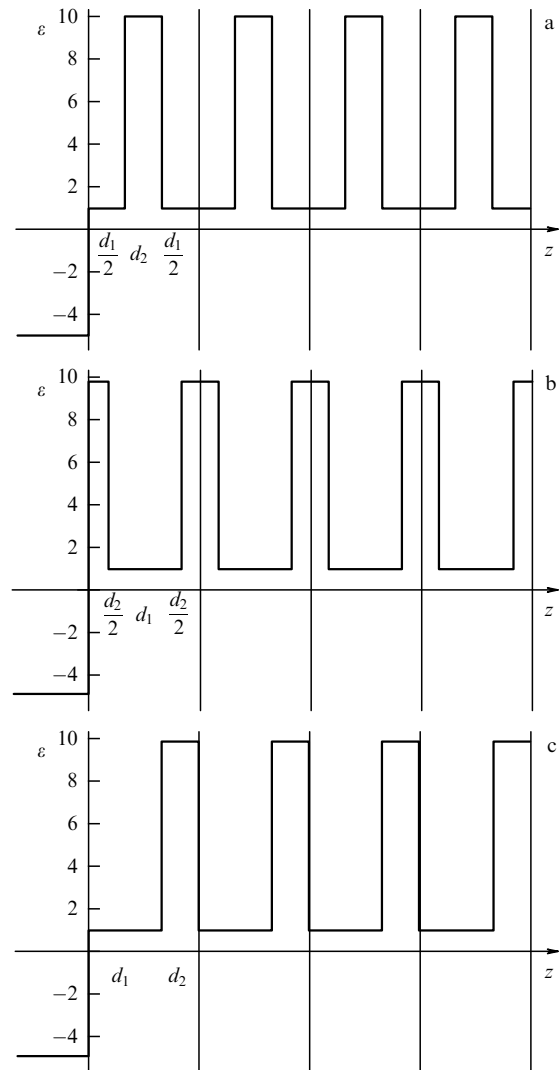

Figure 14. Permittivity versus coordinate in a PC bordering a metal layer ($\varepsilon_{\text{ext}} < 0$) for a symmetric (a, b) and asymmetric (c) cell.

As shown in Ref. [63], Shockley's requirement for the absence of perturbations at the boundary amounts to the requirement that the elementary cell of a crystal be symmetric. The elementary cell used in Tamm's work was taken to be asymmetric with respect to its central plane. [6] Shockley used a symmetric representation of the elementary cell. In the consideration of a semi-infinite space filled with an integer number of elementary cells, passing from the Tamm case to the Shockley case is effected by adding an extra layer at the boundary. In a semi-infinite sample consisting of asymmetric cells, it is indeed possible to recognize a sequence of symmetric cells, and in this case, a part of the asymmetric elementary cell remains on the crystal boundary, which seems like an additional 'potential perturbation at the boundary' (Fig. 14c). Shockley treated this effect as a violation of periodicity. Later, this effect was treated as a perturbation

---

[5] In what follows, we assume that an NP medium is located to the left of a PC.

[6] In particular, the Kronig–Penney potential, which corresponds to a two-layer PC cell, may be represented as symmetric when we consider the elementary cell as one of the layers edged by halves of the other layer. Shockley's requirements for the symmetry of the system then coincide with the requirement that the system comprise an integer number of cells (Figs 14a and 14b).

of the potential at the crystal boundary. As a result, the Tamm states were accidentally attributed to the existence of a perturbation of the potential near the surface [62, 71–74]. The same classification was transferred to photonic crystals [23–25]. Because all the difference between Tamm and Shockley states within this approach reduces merely to the choice of elementary cell representation, this classification of SSs is too farfetched in our view.

However, because the division of SSs into Tamm and Shockley states is widely used, we trace this approach back to its source. By analogy with how it was done in Shockley's paper, we follow the evolution of the band structure and surface states as the distance between 'atoms' varies. In our case, the role of atoms is played by the layers with a high permittivity ε_2.[7] Layers with a permittivity ε_1 ($\varepsilon_1 < \varepsilon_2$) act as the interatomic spacing, with their thickness d_1 being varied. Increasing the interatomic distance in Shockley's work resulted in the emergence of electron tunneling segments. We therefore consider two cases that correspond to positive and negative values of ε_1. The band structure and the location of surface states in both cases are depicted in Fig. 15.

We first consider the case of above-barrier scattering, which occurs in Shockley's model when the atoms are sufficiently close to one another and the electron energy is above the potential inside the lattice. For a PC, this means that $0 < \varepsilon_1 < \varepsilon_2$. We characterize the elementary cell structure by the previously introduced parameter D_1, considering that for $\gamma = k_x/k_0 = 0$, this parameter is

$$D_1 = \frac{d_1\sqrt{\varepsilon_1}}{d_1\sqrt{\varepsilon_1} + d_2\sqrt{\varepsilon_2}}.$$

The frequency is measured in units of $K_0 = \pi/(d_2\sqrt{\varepsilon_2})$. The Bragg condition $k_0(d_1\sqrt{\varepsilon_1} + d_2\sqrt{\varepsilon_2}) = \pi n$ is described by a linear dependence of the frequency k_0 on D_1: $k_0/K_0 = n(1 - D_1)$. The point $d_1 = \infty$ corresponds to $D_1 = 1$; for $k_0 = 0$, this is the point of a zero forbidden band for all n. The condition for the transformation of the nth forbidden band to the zeroth one, $d_1\sqrt{\varepsilon_1}k_0 = \pi n_1$, $d_2\sqrt{\varepsilon_2}k_0 = \pi n_2$, $n = n_1 + n_2$, can be written as

$$D_1 = \frac{n_1/n_2}{1 + n_1/n_2} = \frac{n_1}{n_1 + n_2} = \frac{n_1}{n}, \quad 0 \leqslant n_1 \leqslant n.$$

In other words, the zeroth forbidden band points divide the segment $0 \leqslant D_1 \leqslant 1$ into n equal parts. Each of these sections, which start from and end with a point of a zeroth forbidden band, is referred to as the existence domain of the nth forbidden band. Figure 15a shows the evolution of the band structure with varying D_1: the allowed band domains are shown in grey and the surface states of the PC with the symmetric cell (as in Fig. 14a) are represented by continuous bold lines.

In passing through the zeroth forbidden band points, the imaginary part of the Bloch wavenumber passes through zero and changes sign, while the impedance sign remains unchanged. As a result, the solution that decreases in the PC-inward direction becomes increasing (the solid lines in

[7] For simplicity, we consider the surface state at one boundary of a semi-infinite PC rather than at the two boundaries of a finite crystal, as in Shockley's paper. It is noteworthy that the band structure is independent of the elementary cell representation: symmetric and asymmetric cell representations yield the same band structure.
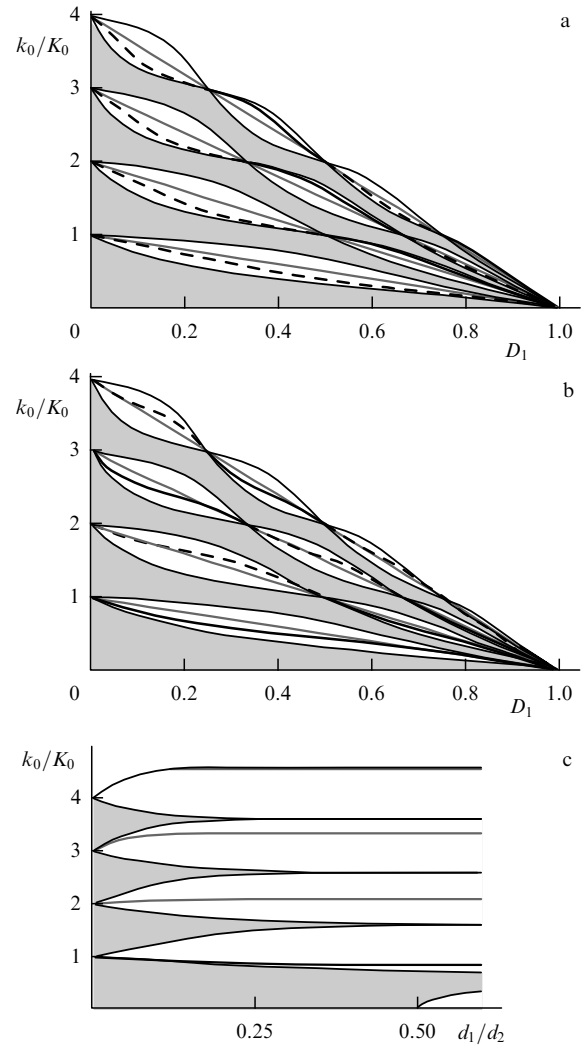

Figure 15. Evolution of the PC band structure with varying d_1 (the distance between the 'atoms'). The allowed bands are marked in grey. The black curves in forbidden bands correspond to surface states. (a) above-barrier reflection ($0 < \varepsilon_1 < \varepsilon_2$). Plotted on the axis is the quantity $D_1 = d_1\sqrt{\varepsilon_1}/(d_1\sqrt{\varepsilon_1} + d_2\sqrt{\varepsilon_2})$, which varies from 0 to 1 as d_1 changes from 0 to ∞. A symmetric PC cell has the form $\{(\varepsilon_1, d_1/2), (\varepsilon_2, d_2), (\varepsilon_1, d_1/2)\}$, $\varepsilon_1 = 1$, $\varepsilon_2 = 10$, $\varepsilon_{ext} = -5$. The lines in the forbidden bands correspond to the equality of the impedances of the wave in the PC and the decaying wave in an NP medium. Solid lines correspond to surface states and dashed lines denote waves that increase in the PC-inward direction. (b) The same for a PC with the cell $\{(\varepsilon_2, d_2/2), (\varepsilon_1, d_1), (\varepsilon_2, d_2/2)\}$. (c) Tunneling ($\varepsilon_1 < 0 < \varepsilon_2$). An asymmetric PC cell has the form $\{(\varepsilon_2, 0.8d_2), (\varepsilon_1, d_1), (\varepsilon_2, 0.2d_2)\}$, $\varepsilon_1 = 1$, $\varepsilon_2 = -2$, $d_2 = 1$, $\varepsilon_{ext} = -5$. There are no surface states in the symmetric case. The frequency is normalized by $K_0 = \pi/(d_2\sqrt{\varepsilon_2})$ in all plots.

Fig. 15a turn into dashed lines) and the SS vanishes, because the NP-medium impedance sign does not change (see Fig. 15).

For a PC with a symmetric cell, the SS evolution curve may enter the domain of forbidden bands only at a zeroth forbidden band (FB) point. Indeed, a symmetric-cell input impedance corresponding to any other point of the boundary is equal to 0 or ∞ (Fig. 16), and therefore the impedances may not be equal for a finite and nonzero value of ε_{ext} for the medium adjacent to the crystal.

For a symmetric cell, therefore, the curve that describes the evolution of the surface state frequency under changes in the cell structure goes in and out of the zeroth FB points
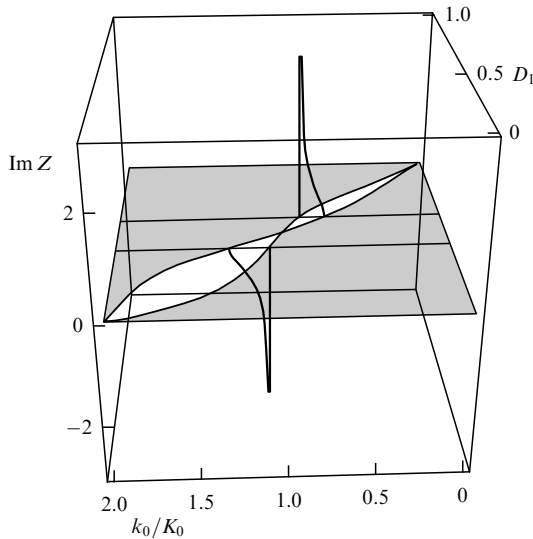
Figure 16. Imaginary part of the input impedance of a wave which decreases away from the boundary of a PC with a symmetric elementary cell for different values of $D_1 = d_1 \sqrt{\varepsilon_1}/(d_1 \sqrt{\varepsilon_1} + d_2 \sqrt{\varepsilon_2})$. The second forbidden band is shown in white. Other forbidden bands (see Fig. 15a) are not shown.

(Fig. 15a) (to be compared with the intersection of s- and p-bands according to Shockley). In this case, surface states are present only in the even domains of existence of forbidden bands (the Shockley FBs according to Klos's terminology [72]). According to [72], the existence domains of forbidden bands without surface states are termed Tamm's domains, and an SS may emerge in them only under a perturbation of the surface potential. We emphasize that this classification is unambiguous only in Shockley's formulation, whereby an atom remains 'indivisible.' In terms of the Kronig–Penney problem with rectangular wells, which is physically realized in semiconductor superlattices and PCs, the 'indivisibility' of an atom corresponds to the 'indivisibility' of the higher-permittivity layer. For such a crystal, the symmetric cell has the form $\{(\varepsilon_2, d_2/2), (\varepsilon_1, d_1), (\varepsilon_2, d_2/2)\}$, and an asymmetric elementary cell representation can then be written as $\{(\varepsilon_2, d_3), (\varepsilon_1, d_1), (\varepsilon_2, (d_2 - d_3))\}$, $0 \leqslant d_3 \leqslant d_2$. Only a part of the possible representations of the PC elementary cell is considered in this approach. By allowing the cell boundary to divide the 'atom' into parts, we obtain an additional set of cells: $\{(\varepsilon_1, d_3), (\varepsilon_2, d_2), (\varepsilon_1, d_1 - d_3)\}$, $0 \leqslant d_3 \leqslant d_1$, with the symmetric cell $\{(\varepsilon_1, d_1/2), (\varepsilon_2, d_2), (\varepsilon_1, d_1/2)\}$. Surface states are now present only in odd domains of existence of forbidden bands, which were previously referred to as Tamm's domains and should now be termed Shockley's [72] (cf. Figs 15a and 15b).

We now consider the PC boundary position corresponding to the asymmetric representation of a binary cell. The cell type is characterized by a parameter α: $\{(\varepsilon_1, (1 - \alpha) d_1/2), (\varepsilon_2, d_2), (\varepsilon_1, (1 + \alpha) d_1/2)\}$. For $\alpha = 0$, we have a symmetric representation with the second layer edged with two halves of the first layer (Fig. 14a), and for $\alpha = \pm 1$, the cell consists of two neighboring layers (Fig. 14b). Clearly, the band structure is independent of α, but the surface state frequencies depend on α because the impedance of the wave in the crystal varies inside the cell (see, e.g., Fig. 3).

For small α, the curve describing the surface state evolution remains qualitatively the same as in the symmetric

cell case: it lies completely inside the Shockley forbidden bands. On transition through some critical value of α, 'phase transitions' commence at the point $D_1 = 1$: in forbidden bands with even numbers, where an SS existed, the evolution curve detaches from the point $D_1 = 1$ (the right point of the zeroth FB) and its right end begins to slide along the FB domain boundary toward the left point of the zeroth FB (the second FB in Fig. 17a); in the bands where no SS existed, the SS evolution curve emerges from the point $D_1 = 1$ and its left end begins to slide along the boundary of the domain of forbidden bands (the first FB in Fig. 17b). As α increases further, motion occurs toward the point $D_1 = 0$, with the different FD domains passed through according to the same scenario: in the domains where SSs existed, they gradually disappear, and in the domains void of SSs, they gradually make their appearance (the second FB in Fig. 17b). In this case, first, each domain of existence of forbidden bands contains at most one evolution curve, which emerges from the zeroth FB point, as in the symmetric cell case. As can be seen from the frequency dependence of the impedance in the asymmetric cell case, precisely one curve emerges from every such point. Second, this process is inherently manifold: there exist several critical parameters α that trigger the process out of the point $D_1 = 1$.

The states that are formed at the asymmetric cell boundary and lie in the 'Tamm' (according to Klos) FB domains are commonly referred to as Tamm states. To be more precise, these states would be more correctly termed non-Shockley states, because these Tamm states and Shockley states arise due to the same formation mechanism, the one proposed in Tamm's works. The division of Tamm states into Shockley and non-Shockley states is related to their evolution rather than the physics of their formation.

We next consider the case of subbarrier transmission, when a PC consists of alternating layers of a dielectric and an
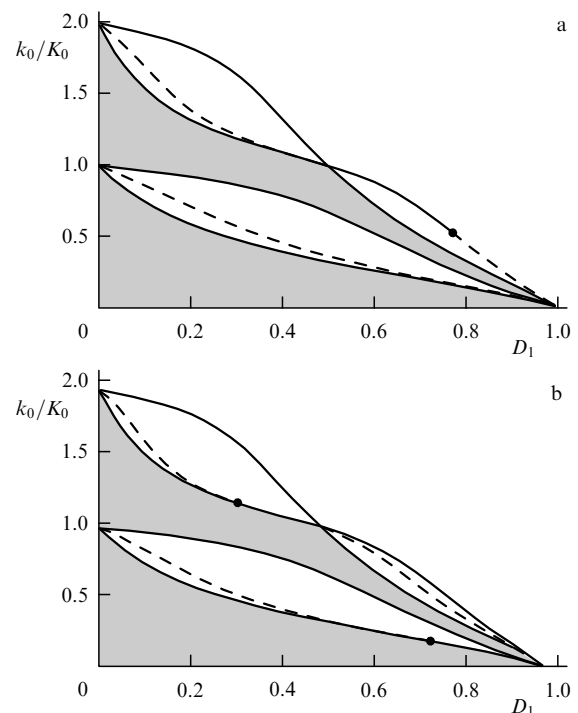

Figure 17. Evolution of surface states due to the disappearance of the central symmetry of the cell: (a) $\alpha = 0.150$, (b) $\alpha = 0.508$.

NP medium.[8] The NP-medium layer corresponds to a long interatomic distance in the Shockley model, with the atom energies lying in the domain of the discrete spectrum. Surface states may then exist only in an asymmetric PC, where the atom-imitating layer is divided. Naturally, a 'part' of the atom appears only at the PC boundary; inside the PC, it joins its complement. It is likely that this fact led Shockley to the statement that the formation of a Tamm SS necessitates the existence of a 'defect' atom on the boundary. From our standpoint, it would be strange to apply the term 'Tamm' to only these states because both cases, tunneling and above-barrier transmission, were considered in Tamm's work.

Therefore, all surface states that form at the PC–NP-medium interface are of the same nature: they decrease both in the PC-inward direction owing to the existence of a forbidden band and inside the NP medium due to the purely imaginary value of the wavenumber, and the frequency corresponds to the condition that the surface impedances are equal.

6. The case of anisotropic photonic crystals

Unlike in Schrödinger quantum mechanics, where the electron behavior is described by a scalar psi-function, the fields in electrodynamics are described not by a scalar but by several vectors, which manifests itself, for instance, in the absence of s-scattering in optics. The direction of these vectors (polarization) may have a qualitative effect on the propagation of electromagnetic waves. In the case of normal incidence of electromagnetic waves on a layered structure, all states are doubly degenerate: both polarizations have the same wave vectors, and the problem reduces to a scalar one, as discussed in Section 3. When the material of one of the elementary cell layers is an anisotropic crystal (which we assume uniaxial for simplicity) and the anisotropy axis is parallel to the layer, the degeneracy is removed and two Bloch waves exist, ordinary and extraordinary. Each of these Bloch waves is a solution of the corresponding independent subsystem of Maxwell equations. It is significant that the boundary conditions are also separated. Due to the independence of the subsystems and boundary conditions, a possible intersection of the dispersion curves of these Bloch waves does not lead to their interaction and hybridization,[9] nor does it lead to the splitting of dispersion curves at their intersection point (Fig. 18).

The removal of degeneracy does not lead to a qualitative change in the band structure. For each polarization, alteration of the allowed and forbidden bands is observed. The forbidden bands are located at the boundaries of Brillouin zones. The forbidden bands corresponding to Bloch waves of different polarizations do not coincide, although they may intersect.

The situation radically changes when isotropic layers are replaced with gyrotropic ones. For clarity, we consider magnetization of a PC in the direction perpendicular to the layers. We assume that the elementary cell of this PC consists of an isotropic magnetooptical layer (the magnetizing field is
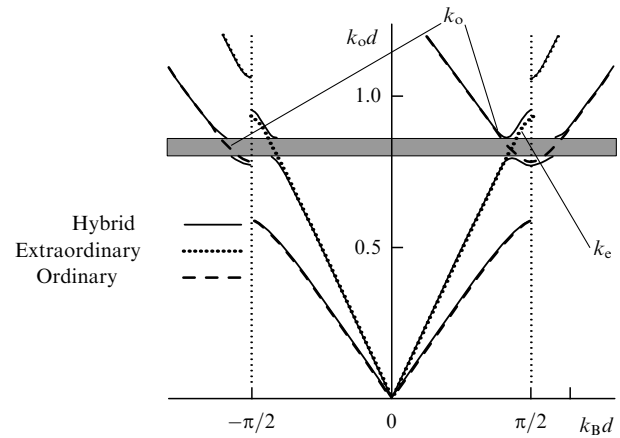

Figure 18. Dispersion curves of ordinary and extraordinary Bloch waves in a PC made of isotropic and anisotropic layers, and the result of hybridization under the emergence of gyrotropic properties in isotropic layers. The PC period consists of a uniaxial crystal with permittivities $\varepsilon_{xx} = 2.0$ and $\varepsilon_{yy} = 8.0$ in the direction of the principal axes and a magnetooptical layer with the permittivity $\varepsilon_{\mathrm{diag}} = 3.0$, $\varepsilon_{\mathrm{off\text{-}diag}} = \mathrm{i}\alpha = 0.5\mathrm{i}$. For clarity, the matter parameters (for instance, the gyrotropy) are artificially exaggerated.

perpendicular to the layers) and an anisotropic layer (the anisotropy axis is parallel to the layers). Prior to magnetization, the magnetooptical layer is an isotropic dielectric with a permittivity ε_{d}; after magnetization, it becomes gyrotropic and its permittivity becomes a tensor of the form

$$\varepsilon = \left\| \begin{array}{ccc} \varepsilon_{\mathrm{d}} & -\varepsilon_{\mathrm{off}} & 0 \\ \varepsilon_{\mathrm{off}} & \varepsilon_{\mathrm{d}} & 0 \\ 0 & 0 & \varepsilon_{\mathrm{d}} \end{array} \right\|.$$

Prior to magnetization, two Bloch waves — ordinary (linearly polarized in the direction perpendicular to the anisotropy axis) and extraordinary (linearly polarized along the anisotropy axis) — could propagate through the PC in the direction perpendicular to the layers. After magnetization, the ordinary and extraordinary waves are no longer eigensolutions for all PC layers, because they are not eigensolutions for the gyrotropic layer. In these layers, the eigensolutions are circularly polarized waves [52]. Clearly, boundary conditions at the layer interfaces mix circularly polarized waves in the magnetooptical layer with linearly polarized waves in the anisotropic layer.[10] The mixing of different solutions at the layer boundaries has the effect that dispersion curves reconnect at the intersection point of the dispersion curves of the ordinary and extraordinary waves of the corresponding nonmagnetized crystal (see Fig. 18). A forbidden band is formed in this case, which may lie not on the boundary but inside the Brillouin zone [76–80]. A similar forbidden band is observed in Solc's periodic filter. This crystal is a PC with the period formed by two different anisotropic uniaxial materials whose axes are parallel to the layers but form an angle with each other [75, 81–84].

This forbidden band forms simultaneously for all solutions,[11] while the location of the FBs formed in the

---

[8] In optics, noble metals may fulfill the function of an NP medium.

[9] We consider linear equations and of course no 'interaction' in terms of nonlinear physics may occur. Interaction in terms of the theory of coupled modes occurs when the initially independent subsystems are coupled. This approach and terminology were elaborated in the pioneering work by Zengerle [75].

[10] We note that neither circularly nor elliptically polarized waves can propagate through an anisotropic crystal.

[11] Here, we do not distinguish solutions by polarization, because there is no way to unambiguously define the notion of polarization for a hybridized Bloch wave (see Ref. [85]).
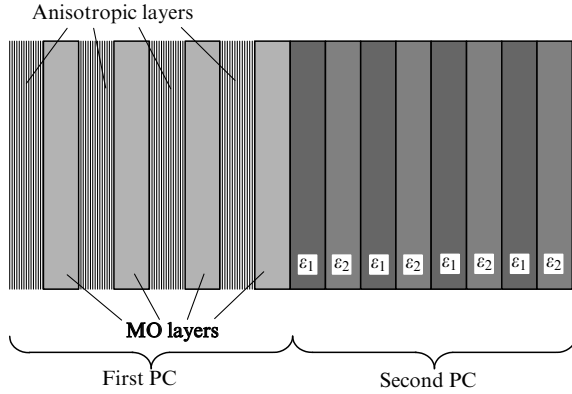
Figure 19. System of two PCs in which Tamm's state is observed inside the Brillouin zone of one of them. The period of the first PC consists of a uniaxial crystal with the permittivity $\varepsilon_{xx} = 2.7$, $\varepsilon_{yy} = \varepsilon_{zz} = 5.0$ in the directions of the principal axes and a magnetooptical (MO) layer with the permittivity $\varepsilon_{xx} = \varepsilon_{yy} = \varepsilon_{zz} = 3.0$, $\varepsilon_{xy} = -\varepsilon_{yx} = i\alpha = 0.02i$. The layer permittivity values in the second PC are $\varepsilon_1 = 3.1$ and $\varepsilon_1 = 3.1$, $\varepsilon_2 = 3.4$. All layers have the same thickness of 100 nm.

Brillouin boundary may depend on the choice of the solution polarization (see Fig. 18). In other words, the formation of additional bands is degenerate with respect to polarization [85], and these bands are referred to as degenerate. It is significant that the true degeneracy — the equality of the wave vectors (reduced to the first Brillouin zone) of different waves — occurs only at the boundary of a degenerate FB. For the frequencies inside this band, the Bloch vector has a special form for four solutions (two forward and two backward): $k_{1,2}(k_0) = \pm(a(k_0) + ib(k_0))$ and $k_{3,4}(k_0) = \pm(a(k_0) - ib(k_0))$ [85].

The formation of a degenerate FB under magnetization allows controlling the emergence of Tamm's states.

We consider a system consisting of two finite one-dimensional photonic crystals (Fig. 19). The period of the first PC consists of an anisotropic layer and a magnetooptical one. The period of the second PC consists of two isotropic layers. We consider the frequencies near the intersection of the dispersion curves of the first PC. It is assumed that the intersection point lies in the allowed band in the absence of magnetization and that this frequency lies in the FB of the second PC. Prior to applying the magnetic field, the transmission through the system is suppressed due to the existence of the FB in the second PC (Fig. 20).

Application of the magnetic field gives rise to an FB in the first PC [85] (see the solid line in Fig. 20b) and the consequential formation of a Tamm state at the boundary between the two PCs. This Tamm state manifests itself as a sharp peak in the transmission spectrum (see Fig. 20) [77].

Unlike the Tamm state in a magnetophotonic crystal (MPC) involving isotropic components, considered in Sections 4 and 5, a Tamm state does not split here into two states with different frequencies after application of the magnetic field, but simply emerges. The state is not doubly degenerate in polarization, as with a PC involving isotropic components (in an MPC without magnetization); as a result, there is one Tamm state, which does not split in the magnetic field. This feature stems from the hybridization of solutions in inhomogeneous magnetic materials containing anisotropic components.

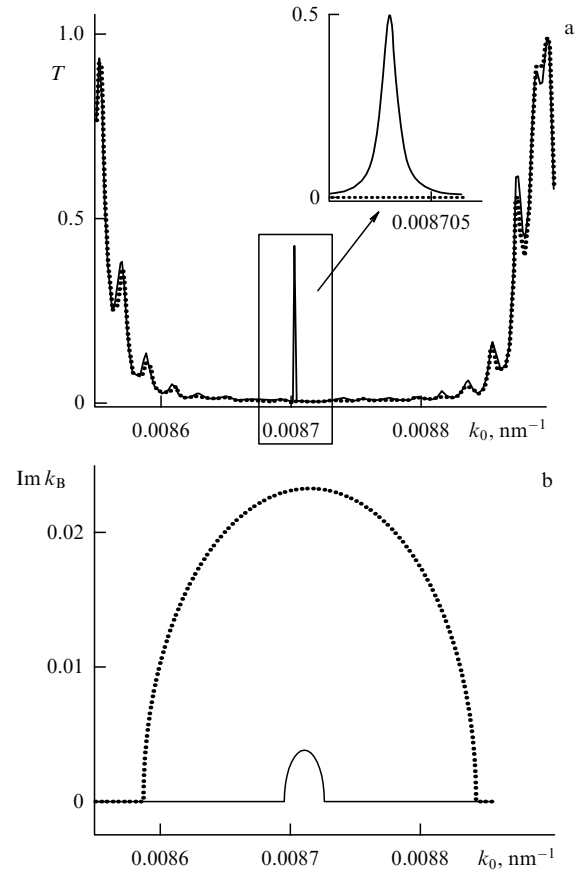The fundamental difference between hybrid and non-hybrid solutions is as follows: when hybridization is absent,

Figure 20. (a) Two-PC system transmittance (see Fig. 19) in the absence (curve with circles) and in the presence (solid curve) of magnetization. (b) Imaginary part of the Bloch wavenumber of an ordinary (curve with circles) and magnetooptical (solid curve) PC in the presence of magnetization. The parameters of the samples are the same as in Fig. 19.

it is possible to distinguish the solutions by polarization (circularly right- and left-polarized, TE and TM modes, and so on) and thus reduce the vector problem to two independent scalar problems. To match the eigensolutions, it is possible to introduce scalar (isotropic) input admittances, whose equality ensures the matching. The solution mixing at layer boundaries results in the Bloch wave in each layer consisting of four waves, which have different polarizations and propagate in opposite directions. This solution is commonly referred to as hybrid, because it does not consist only of waves of a specific polarization. A characteristic feature of the hybrid Bloch solution is that it has an anisotropic admittance.

We consider the structure of the hybrid solution in an anisotropic layer. In the general case, the solution in an anisotropic layer can be written as

$$\mathbf{E} = \begin{pmatrix} E_x \\ E_y \end{pmatrix} = A \begin{pmatrix} 1 \\ 0 \end{pmatrix} \exp(ik_o z) + B \begin{pmatrix} 1 \\ 0 \end{pmatrix} \exp(-ik_o z)$$
$$+ C \begin{pmatrix} 0 \\ 1 \end{pmatrix} \exp(ik_e z) + D \begin{pmatrix} 0 \\ 1 \end{pmatrix} \exp(-ik_e z),$$

where A, B, C, and D are the amplitudes of the corresponding four plane waves that are solutions of the Maxwell equations in the layer under consideration, k_o is the wave vector of the ordinary wave, and k_e is the wave vector of the extraordinary wave. At the interface between the anisotropic–gyrotropic PC

and the PC with isotropic components, we should match the tangential components of the electric and magnetic fields, i.e., the four components E_x, E_y, H_x, and H_y. Interestingly, when it is required to solve an eigenvalue problem instead of a scattering problem with a fixed incident wave amplitude, it suffices to match not the absolute field values but simply their ratios $Y_x = H_x/E_y$ and $Y_y = -H_y/E_x$ (in quantum mechanics, this corresponds to matching the logarithmic derivative). The quantities Y have the meaning of the input admittances. For any isotropic medium, its admittance is isotropic, i.e., $Y_x = H_x/E_y = k/k_0 = -H_y/E_x = Y_y$, which directly follows from the equation $\mathrm{curl}\,(\mathbf{E}) = (1/c)\,\mathrm{d}\mathbf{H}/\mathrm{d}t$. For one hybrid wave, the admittances are not equal because

$$Y_x = \frac{H_x}{E_y} = \frac{k_1}{k_0} \neq \frac{k_2}{k_0} = -\frac{H_y}{E_x} = Y_y\,,$$

in the anisotropic layer, and therefore a single eigensolution in the anisotropic–gyrotropic PC cannot be matched to the solution in the PC with isotropic components; the solution in the anisotropic–gyrotropic PC must be sought in the form of the sum of two damped modes (with different wave vectors) $k_1(k_0) = a(k_0) + ib(k_0)$ and $k_4(k_0) = -a(k_0) + ib(k_0)$:

$$\mathbf{E} = A\begin{pmatrix} f_{1x}\,(z) \\ f_{1y}\,(z) \end{pmatrix} \exp\,(ik_1 z) + B\begin{pmatrix} f_{2x}\,(z) \\ f_{2y}\,(z) \end{pmatrix} \exp\,(ik_2 z)\,.$$

Accordingly, the magnetic field is

$$\mathbf{H} = A\begin{pmatrix} Y_{1y}f_{1y}\,(z) \\ -Y_{1x}f_{1x}\,(z) \end{pmatrix} \exp\,(ik_1 z)$$
$$+ B\begin{pmatrix} Y_{2y}f_{2y}\,(z) \\ -Y_{2x}f_{2x}\,(z) \end{pmatrix} \exp\,(ik_2 z)\,,$$

where

$$Y_{\alpha\beta} = n_\alpha + \frac{f'_{\alpha\beta}}{f_{\alpha\beta}\,ik_0}\,,$$

$\alpha = 1, 2$ is the solution number and the subscript $\beta = x, y$ indicates the corresponding component.

By equating the corresponding field components in the anisotropic MPC to the fields in the PC with isotropic components at the PC interface (which is taken as the origin),

$$\mathbf{E} = \begin{pmatrix} E_x \\ E_y \end{pmatrix} = \begin{pmatrix} af\,(z) \\ bf\,(z) \end{pmatrix} \exp\,(ikz)\,,$$

$$\mathbf{H} = \begin{pmatrix} H_x \\ H_y \end{pmatrix} = \begin{pmatrix} b\left(n + \dfrac{f'}{f\,ik_0}\right)f \\ -a\left(n + \dfrac{f'}{f\,ik_0}\right)f \end{pmatrix} \exp\,(ikz)\,,$$

we obtain the system of equations

$$A\begin{pmatrix} f_{1x} \\ f_{1y} \end{pmatrix} + B\begin{pmatrix} f_{2x} \\ f_{2y} \end{pmatrix} = \begin{pmatrix} af \\ bf \end{pmatrix}\,,$$

$$A\begin{pmatrix} Y_{1y}f_{1y} \\ -Y_{1x}f_{1x} \end{pmatrix} \exp\,(ik_1 z) + B\begin{pmatrix} Y_{2y}f_{2y} \\ -Y_{2x}f_{2x} \end{pmatrix} = \begin{pmatrix} bYf \\ -aYf \end{pmatrix}\,.$$

We derive expressions for $af\,(z)$ and $bf\,(z)$ from the first equation and substitute them in the second to obtain

$$A(Y_{1y} - Y)f_{1y} + B(Y_{2y} - Y)f_{2y} = 0\,,$$

$$A(Y_{1x} - Y)f_{1x} + B(Y_{2x} - Y)f_{2x} = 0\,.$$

This system has a nontrivial solution only when its determinant is equal to zero:

$$\begin{vmatrix} (Y_{1y} - Y)f_{1y} & (Y_{2y} - Y)f_{2y} \\ (Y_{1x} - Y)f_{1x} & (Y_{2y} - Y)f_{2x} \end{vmatrix} = 0\,.$$

It is precisely this expression instead of the usual equality of impedances that defines the position of the Tamm resonance.

7. Conclusion

As with electronic crystals, the existence of surface states in PCs is related to a significant variation of Bloch functions on the elementary cell scale. In this case, the input impedance changes significantly with changes in the PC boundary relative to the elementary cell, as well as with frequency variation inside the forbidden band (see Fig. 16), making it possible to match the solution not only to solutions for NP and NMP media but also to a solution for another PC that has a forbidden band. At forbidden band frequencies, a PC may manifest itself as a medium with positive magnetic permeability and negative permittivity or as a medium with positive permittivity and negative magnetic permeability, and therefore the SS formed at the interface between two PCs may be considered an analogue of the SS emerging at the interface between NP and NMP media [36].

The SS localization at the PC interface is due to the attenuation of the Bloch wave in the PC-inward direction at forbidden band frequencies, which is exponential on average. In accordance with this SS formation mechanism, all SSs at PC boundaries are Tamm's SSs. The division of Tamm's states into Shockley and non-Shockley states is related not to the physical nature of these states but to the symmetry of the elementary cell. This division manifests itself only in the consideration of band structure evolution under the variation of PC parameters and has no fundamental importance for a specific PC.

References

1. Joannopoulos J D, Meade R D, Winn J N *Photonic Crystals: Molding the Flow of Light* (Princeton, NJ: Princeton Univ. Press, 1995)
2. Johnson S G, Joannopoulos J D *Photonic Crystals: The Road from Theory to Practice* (Boston: Kluwer Acad. Publ., 2002)
3. Sakoda K *Optical Properties of Photonic Crystals* (Berlin: Springer, 2001)
4. Silin R A *Neobychnye Zakony Prelomleniya i Otrazheniya* (Unusual Laws of Refraction and Reflection) (Moscow: FAZIS, 1999)
5. Luo C et al. *Phys. Rev. B* **65** 201104(R) (2002)
6. Russell P St J, Birks T A, in *Photonic Band Gap Materials* (Ed. C M Soukoulis) (Dordrecht: Kluwer Acad. Publ., 1996) p. 71
7. Kosaka H et al. *Phys. Rev. B* **58** R10096 (1998)
8. Baba T, Matsumoto T *Appl. Phys. Lett.* **81** 2325 (2002)
9. Merzlikin A M, Vinogradov A P *Opt. Commun.* **259** 700 (2006)
10. Belov P A, Simovski C R, Ikonen P *Phys. Rev. B* **71** 193105 (2005)
11. Chuprunov E V, Khokhlov A F, Faddeev M A *Osnovy Kristallografii* (Foundations of Crystallography) (Moscow: Fizmatlit, 2004)
12. Batterman B W, Cole H *Rev. Mod. Phys.* **36** 681 (1964)
13. Zhang Z, Satpathy S *Phys. Rev. Lett.* **65** 2650 (1990)
14. Tikhodeev S G et al. *Phys. Rev. B* **66** 045102 (2002)
15. John S *Phys. Rev. Lett.* **58** 2486 (1987)
16. Berry M V, Popescu S *J. Phys. A Mat. Gen.* **39** 6965 (2006)

17. Berry M V *J. Phys. A Mat. Gen.* **27** L391 (1994)
18. Kempf A, Ferreira P J S G *J. Phys. A Mat. Gen.* **37** 12067 (2004)
19. Ferreira P J S G, Kempf A *IEEE Trans. Signal Process.* **54** 3732 (2006)
20. Tamm I *Z. Phys.* **76** 849 (1932)
21. Shockley W *Phys. Rev.* **56** 317 (1939)
22. Landau L D, Lifshitz E M *Elektrodinamika Sploshnykh Sred* (Electrodynamics of Continuous Media) (Moscow: Nauka, 1982) [translated into English (Oxford: Pergamon Press, 1984)]
23. Klos J *Phys. Rev. B* **76** 165125 (2007)
24. Malkova N, Ning C Z *Phys. Rev. B* **73** 113113 (2006)
25. Malkova N, Ning C Z *Phys. Rev. B* **76** 045305 (2007)
26. Agranovich V M, Mills D L (Eds) *Surface Polaritons: Electromagnetic Waves at Surfaces and Interfaces* (Amsterdam: North-Holland, 1982) [Translated into Russian (Moscow: Nauka, 1985)]
27. Dmitruk N L, Litovchenko V G, Strizhevskii V L *Poverkhnostnye Polyaritony v Poluprovodnikakh i Dielektrikakh* (Surface Polaritons in Semiconductors and Dielectrics) (Kiev: Naukova Dumka, 1989)
28. Alu A, Engheta N *IEEE Trans. Antennas Propag.* **51** 2558 (2003)
29. Zouhdi S et al. *Phys. Rev. B* **75** 035125 (2007)
30. Vainshtein L A *Elektromagnitnye Volny* (Electromagnetic Waves) 2nd ed. (Moscow: Radio i Svyaz', 1988)
31. Yariv A, Yeh P *Optical Waves in Crystals* (New York: Wiley, 1984) [Translated into Russian (Moscow: Mir, 1987)]
32. Brekhovskikh L M *Volny v Sloistykh Sredakh* (Waves in Layered Media) (Moscow: Izd. AN SSSR, 1957) [Translated into English (New York: Academic Press, 1960)]
33. Rytov S M *Zh. Eksp. Teor. Fiz.* **29** 606 (1955) [*Sov. Phys. JETP* **2** 466 (1956)]
34. Bass F G, Bulgakov A A, Tetervov A P *Vysokochastotnye Svoistva Poluprovodnikov so Sverkhreshetkami* (High-Frequency Properties of Semiconductors with Superlattices) (Moscow: Nauka, 1989)
35. Kronig R, Penney W G *Proc. R. Soc. London A* **130** 499 (1931)
36. Vinogradov A P et al. *Phys. Rev. B* **74** 045128 (2006)
37. Namdar A, Shadrivov I V, Kivshar Yu S *Appl. Phys. Lett.* **89** 114104 (2006)
38. Barvestani J et al. *Phys. Rev. A* **77** 013805 (2008)
39. Namdar A, Shadrivov I V, Kivshar Yu S *Phys. Rev. A* **75** 053812 (2007)
40. Bass F G, Tetervov A P *Phys. Rep.* **140** 237 (1986)
41. Kaliteevski M et al. *Phys. Rev. B* **76** 165415 (2007)
42. Tamm I *Phys. Z. Sowjetunion* **1** 733 (1932)
43. Lifshits I M, Pekar S I *Usp. Fiz. Nauk* **56** 531 (1955)
44. Goto T et al. *Phys. Rev. Lett.* **101** 113902 (2008)
45. Kavokin A, Shelykh I, Malpuech G *Appl. Phys. Lett.* **87** 261105 (2005)
46. Kavokin A V, Shelykh I A, Malpuech G *Phys. Rev. B* **72** 233102 (2005)
47. Villa F, Gaspar-Armenta J A *Opt. Commun.* **223** 109 (2003)
48. Villa F, Gaspar-Armenta J *Opt. Express* **12** 2338 (2004)
49. Ji-Yong Guo et al. *Chin. Phys. Lett.* **25** 2093 (2008)
50. Brand S, Kaliteevski M A, Abram R A *Phys. Rev. B* **79** 085416 (2009)
51. Bulgakov A A, Meriutz A V, Ol'khovskii E A *Zh. Tekh. Fiz.* **74** (10) 103 (2004) [*Tech. Phys.* **49** 1349 (2004)]
52. Zvezdin A K, Kotov V A *Magnitooptika Tonkikh Plenok* (Magnetooptics of Thin Films) (Moscow: Nauka, 1988)]
53. Inoue M et al. *J. Appl. Phys.* **83** 6768 (1998)
54. Steel M J, Levy M, Osgood R M (Jr.) *J. Lightwave Technol.* **18** 1297 (2000)
55. Goodwin E T *Proc. Camb. Philos. Soc.* **35** 205 (1939); **35** 221 (1939); **35** 232 (1939)
56. Maue A-W *Z. Phys.* **94** 717 (1935)
57. Rijanow S *Z. Phys.* **89** 806 (1934)
58. Sokolow A *Z. Phys.* **90** 520 (1934)
59. Sokolov A A *Zh. Eksp. Teor. Fiz.* **6** 807 (1936)
60. Tsenter E M *Zh. Eksp. Teor. Fiz.* **8** 682 (1938)
61. Levine J D *Phys. Rev.* **171** 701 (1968)
62. Davison S G, Levine J D "Surface states", in *Solid State Physics* Vol. 25 (Eds H Ehrenreich, F Seitz, D Turnbull) (New York: Academic Press, 1970) [Translated into Russian: *Poverkhnostnye (Tammovskie) Sostoyaniya* (Moscow: Mir, 1973)]
63. Zak J *Phys. Rev. B* **32** 2218 (1985)
64. Green M (Ed.) *Solid State Surface Science* Vol. 1 (New York: M. Dekker, 1969) [Translated inro Russian (Moscow: Mir, 1972)]
65. Belen'kii A Ya *Usp. Fiz. Nauk* **134** 125 (1981) [*Sov. Phys. Usp.* **24** 412 (1981)]
66. Allen G *Phys. Rev.* **91** 531 (1953)
67. Leyva M D, Gondar J L *Phys. Status Solidi B* **128** 575 (1985)
68. Milanović V, Tjapkin D *Phys. Status Solidi B* **110** 687 (1982)
69. Nusinsky I, Hardy A A *Phys. Rev. B* **73** 125104 (2006)
70. Vinogradov A P, Merzlikin A M *Physica B* **338** 126 (2003)
71. Foo E-N, Wong H-S *Phys. Rev. B* **9** 1857 (1974)
72. Klos J, Puszkarski H *Phys. Rev. B* **68** 045316 (2003)
73. Foo E-N, Wong H S *Phys. Rev. B* **10** 4819 (1974)
74. Stęślicka M et al. *Surf. Sci. Rep.* **47** 93 (2002)
75. Zengerle R *J. Mod. Opt.* **34** 1589 (1987)
76. Merzlikin A M et al. *J. Magn. Magn. Mater.* **300** 108 (2006)
77. Merzlikin A M et al. *Physica B* **394** 277 (2007)
78. Levy M, Jalali A A *J. Opt. Soc. Am. B* **24** 1603 (2007)
79. Jalali A A, Levy M *J. Opt. Soc. Am. B* **25** 119 (2008)
80. Wang F, Lakhtakia A *Appl. Phys. Lett.* **92** 011115 (2008)
81. Šolc I *Czech. J. Phys.* **4** 53 (1954); **4** 65 (1954)
82. Yeh P *J. Opt. Soc. Am.* **69** 742 (1979)
83. Cojocaru E *Appl. Opt.* **39** 4641 (2000)
84. Shabtay G et al. *Opt. Express* **10** 1534 (2002)
85. Merzlikin A M et al. *Phys. Rev. B* **79** 195103 (2009)